

Signature of hidden order in heavy fermion superconductor URu₂Si₂: Resonance at the wave vector $\mathbf{Q}_0=(1,0,0)$

A. Villaume, F. Bourdarot,* E. Hassinger, S. Raymond, V. Taufour, D. Aoki, and J. Flouquet
Institut Nanosciences et Cryogenie, SPSMS/MDN, CEA-Grenoble, 38054 Grenoble, France

(Received 17 June 2008; published 18 July 2008)

Simultaneous neutron scattering and thermal expansion measurements on the heavy-fermion superconductor URu₂Si₂ under hydrostatic pressure of 0.67 GPa have been performed in order to detect the successive paramagnetic, hidden order, and large moment antiferromagnetic phases on cooling. The temperature dependence of the sharp low energy excitation at the wave vector $\mathbf{Q}_0=(1,0,0)$ shows clearly that this resonance is a signature of the hidden order state. In the antiferromagnetic phase, this resonance disappears. The higher energy excitation at the incommensurate wave vector $\mathbf{Q}_1=(1.4,0,0)$ persists in the antiferromagnetic phase but increases in energy.

DOI: 10.1103/PhysRevB.78.012504

PACS number(s): 74.70.Tx, 78.70.Nx, 71.27.+a, 72.15.Qm

The elucidation of the nature of a hidden order in exotic materials, which belong often to the rich class of strongly correlated electronic systems, is a hot subject as it can lead to the discovery of unexpected new order parameters. Debates exist on quite different proposals such as orbital hidden order in the heavy fermion system URu₂Si₂,¹ multipolar ordering in rare earth skutterudites² or “spin order accompanying loop current” in cuprate superconductors.³

Due to the dual character of the 5*f* electrons in URu₂Si₂ between localized (leading to the possibility of multipolar ordering) and itinerant (possibility of large Fermi surface instabilities), this compound has been the subject of a large variety of experiments.⁴ At zero pressure, a phase transition occurs from the paramagnetic (PM) phase to a so-called hidden order (HO) phase at a temperature $T_0 \sim 17.5$ K. The hidden order label reflects the fact that this order may not be of dipolar origin. The order parameter is not yet determined: spin or charge density wave,^{5–7} multipolar ordering,^{8–11} orbital antiferromagnetism,¹ chiral spin state,¹² and helicity order¹³ have been proposed. The long standing debate on the occurrence of a tiny ordered moment $M_0 \sim 0.02\mu_B$ per U atom at $T \rightarrow 0$ K for the antiferromagnetic (AF) wave vector $\mathbf{Q}_{AF}=(0,0,1)$ seems to converge now toward an extrinsic origin directly related to the high sensitivity of URu₂Si₂ to pressure and stress (low critical pressure $P_x \sim 0.5$ GPa).^{4,14–16}

Pressure studies^{4,17–19} reveal an interesting phase diagram (Fig. 1). At $T \rightarrow 0$ K, neutron scattering experiments⁴ show that the hidden-order ground state switches at P_x to a large moment antiferromagnetic (AF) state of sublattice magnetization M_0 near $0.3\mu_B/U$ with a propagation vector \mathbf{Q}_{AF} . The HO-AF boundary $T_x(P)$ meets the $T_0(P)$ line at the tricritical point ($T^* \sim 19.3$ K, $P^* \sim 1.36$ GPa);¹⁹ above P^* , a unique ordered phase (AF) is established below $T_N(P)$. Previous nuclear magnetic resonance (NMR) experiments,^{14,20} as well as transport measurements,^{5,19} indicate clearly that nesting occurs at T_0 , as well as at T_N , indicating also that the Fermi surface is not deeply modified through the transition line T_x .

The interest in URu₂Si₂ is reinforced by the appearance of unconventional superconductivity at $T_{sc} \sim 1.2$ K for $P=0$ (Ref. 21), which disappears in the bulk at P_x .^{4,19}

Up to now, there is no direct convincing microscopic signature of the hidden order state. For example, the previous

claim of residual Si NMR linewidth²² has been rejected;^{15,23} the proposal of orbital antiferromagnetism is not demonstrated.²⁴

The aim of the present work is to clarify the inelastic neutron scattering response for both ordered phases. At $P=0$, two main inelastic magnetic responses of $\mathbf{Q}_{AF}=(0,0,1)$ and of an incommensurate wave vector $\mathbf{Q}_{INC}=(0.4,0,1)$ are detected. These signals are insensitive to annealing conditions by contrast to the temperature dependence of the elastic intensity linked to the residual tiny ordered moment.²⁵ Because of the Ising character along the *c* axis of the magnetic excitations, they have been measured at the equivalent positions $\mathbf{Q}_0=(1,0,0)$ for \mathbf{Q}_{AF} and $\mathbf{Q}_1=(1.4,0,0)$ for \mathbf{Q}_{INC} .^{26–29} The remarkable feature is that below T_0 both excitations are sharp with respective gaps at $\Delta_0=1.8$ meV and $\Delta_1=4.5$ meV.²⁸ Furthermore their temperature evolutions explain the shape of the specific heat anomaly at T_0 .^{29,30} The clear trend is a strong interplay between these two inelastic responses. It was recently suggested that \mathbf{Q}_{INC} may be a wave vector for a spin density wave occurring at T_0 .²⁹ However no evidence is found even in NMR experiments.¹⁵

Previous neutron scattering experiments under pressure

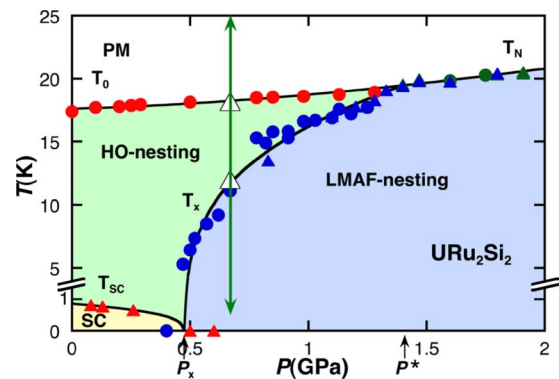


FIG. 1. (Color online) (T, P) phase diagram of URu₂Si₂ from resistivity (circles) and ac calorimetry (triangles) measurements (Ref. 19) with the low-pressure HO phase and the high-pressure AF phase. Bulk superconductivity state is suppressed at P_x when antiferromagnetism appears. The open triangles correspond to the present determination of T_0 and T_x at $P=0.67$ GPa.

have led to suggest that the low-energy excitation characteristic of \mathbf{Q}_0 may collapse at low temperature when entering the antiferromagnetic state;^{25,31,32} but either the accuracy of the data is poor or the pressure condition was not well established (for example, P_x was claimed equal to 1.3 GPa in Ref. 32). Furthermore there are contradictory conclusions for Δ_1 : persistence according to Ref. 31 or collapse according to Ref. 32. In contrast to these previous experiments,^{31,32} where the studies are made at different pressures with no analysis of the temperature dependence, the present choice is to work at a constant pressure $P=0.67$ GPa slightly above P_x . At this pressure, each phase has a significant temperature range of existence as $T_0=18.2$ K and $T_x=12.0$ K. Furthermore, the precise transition temperatures T_0 and T_x have been determined during the neutron scattering experiment by thermal expansion.

The main result of this Brief Report is the simultaneous thermal evolution of the ordered antiferromagnetic moment and of the inelastic intensities of the gaps at \mathbf{Q}_0 and \mathbf{Q}_1 both in the hidden order and antiferromagnetic phases at $P=0.67$ GPa. The hidden order state is associated with a strong inelastic signal at \mathbf{Q}_0 . In the antiferromagnetic phase, the inelastic signal vanishes as the ordered moment appears at \mathbf{Q}_0 . At \mathbf{Q}_1 , a clear inelastic spectrum persists; the gap Δ_1 changes abruptly when entering the antiferromagnetic phase.

Neutron scattering measurements were performed at the Institut Laue-Langevin (ILL) on the IN12 and IN22 cold and thermal triple-axis spectrometers, respectively. The energy resolution determined by the incoherent scan at zero energy transfer was 0.22 meV and 0.9 meV, respectively, on IN12 and IN22 at full width at half maximum. Furthermore, as the IN12 spectrometer is located at the end of the cold neutron guide, the background is far lower than the one in previous pressure experiments.³¹⁻³³ IN22 was used for the studies at \mathbf{Q}_1 in order to reach higher energy. In each case, we used a well-adjusted cadmium shielding around the pressure cell.

A single crystal, grown by the Czochralski method, of size of $\sim 5 \times 4 \times 3$ mm³, from the same batch used in the high-magnetic-field measurements of Ref. 28 and in the previous high-pressure measurements,³¹ was used for the experiment. A flat surface was cleaved perpendicular to the c axis. This axis and one a axis were in the scattering plane.

Measurements under pressure were performed using a homemade CuBe pressure cell. A strain gage (see Ref. 34) was glued along the a axis on the flat surface perpendicular to the c axis. To transmit the pressure, a mixture 1:1 of fluorinert 70 and 77 was used. The pressure-dependent superconducting transition of lead was measured by ac magnetic susceptibility. The pressure conditions are similar to those used in Ref. 4.

The thermal expansion measurements performed at $P=0.67$ GPa indicate transition temperatures of $T_0=18.2$ K and $T_x=12.0$ K (Fig. 2). An excellent agreement is found between these results and the recent determination of the (T,P) phase diagram, as shown in Fig. 1.¹⁹ The precise knowledge of the localization in this phase diagram is an important advantage of this experiment in order to corroborate both thermal expansion and neutron scattering experiments. This was not achieved in the previous experiments.^{31,32} The temperature dependence of the magnetic

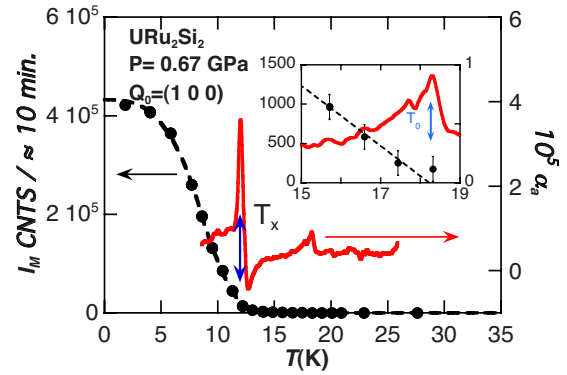


FIG. 2. (Color online) Thermal evolution of the magnetic Bragg peak intensity at $\mathbf{Q}_0=(1,0,0)$ (dashed line) and of the thermal expansion α_a (solid line) of URu_2Si_2 at $P=0.67$ Pa. I_M corresponds to the count at the top of the magnetic Bragg peak \mathbf{Q}_0 per 10 min, the background subtracted. The inset is a zoom of I_M and α_a in the HO phase.

elastic intensity ($I_M \propto M^2$) at \mathbf{Q}_0 is also shown in Fig. 2. The onset of the large elastic antiferromagnetic signal at \mathbf{Q}_0 coincides with the thermal expansion jump at T_x . The estimation of M_0 in the antiferromagnetic phase gives $0.4\mu_B/U$, in agreement with previous results.^{4,18,31,35} A small magnetic intensity survives above T_x and collapses linearly in temperature at T_0 as found in Ref. 18 and 26 but not in Ref. 4. The extrapolation to 0 K of the tiny ordered moment is $0.05\mu_B/U$. This tiny ordered moment is assumed to emanate from the same extrinsic origin as the one at ambient pressure.

A large inelastic signal, coming essentially from the sample as it can be verified on the residual background, is shown in Fig. 3. At \mathbf{Q}_0 , in the paramagnetic regime ($T=20.1$ K), the signal is weak and strongly damped. In the hidden order phase ($T=13.9$ K), an inelastic spectrum similar to the spectrum measured in URu_2Si_2 at $P=0$ with an energy gap $E_0 \sim 1.25$ meV is observed. In the antiferromagnetic state ($T=1.5$ K), neither quasielastic nor inelastic response can be detected at low temperature.

Figure 4 represents the magnetic excitation at the wave vector \mathbf{Q}_1 in the three phases. Above T_0 , the signal is mainly quasielastic and broadened. In the hidden order phase, it be-

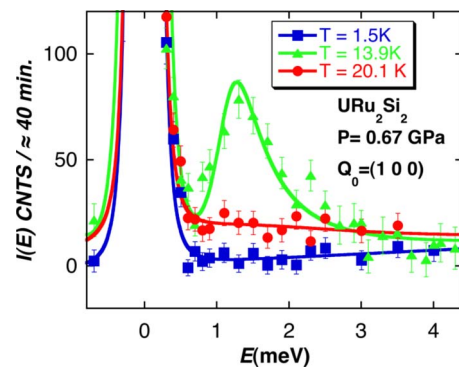


FIG. 3. (Color online) Energy scan at \mathbf{Q}_0 in the PM ($T=20.1$ K), HO ($T=13.9$ K), and AF ($T=1.5$ K) phases. Only electronic background has been subtracted. The curves are guides for the eyes.

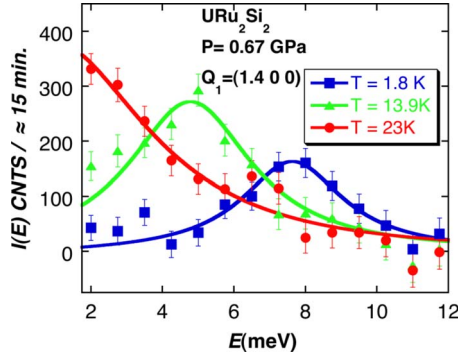


FIG. 4. (Color online) Energy scan at \mathbf{Q}_1 in the PM ($T=20.1$ K), HO ($T=13.9$ K), and AF ($T=1.5$ K) phases. An energy scan measured at $T=1.8$ K at the wave vector $\mathbf{Q}=(1.3,0,0)$ has been used as background and subtracted to the energy scans measured at \mathbf{Q}_1 . The curves are guides for the eyes.

comes mostly inelastic with an energy gap $\Delta_1=5$ meV. This magnetic excitation persists on entering the antiferromagnetic phase but is shifted to 7.8 meV. This shift to higher energy is accompanied by a decrease in the inelastic amplitude (at zero order, I_{Δ_1} varies as $1/\Delta_1$ ²⁹).

In order to precisely characterize the inelastic response at \mathbf{Q}_0 , we performed many scans in the temperature range 1.5 to 33 K. Figure 5 shows $I_{\Delta_0}(\mathbf{Q}_0) \propto \int_{0.6}^{2.5} \text{meV} \chi''(E, \mathbf{Q}_0) dE$, the integration of the dynamic susceptibility at \mathbf{Q}_0 where the magnetic excitation is detected. The width and the position of the inelastic peak at \mathbf{Q}_0 stay constant below T_0 and even through T_x . In the paramagnetic state, the strongly damped signal increases smoothly on approaching T_0 . At T_0 , the intensity rises abruptly. This increase is very similar to the behavior of the integration of the dynamic susceptibility at \mathbf{Q}_0 found in the sample at $P=0$.^{18,27,29} For $P=0.67$ GPa, this intensity reaches a maximum at T_x and then decreases and collapses for $T \rightarrow 0$. The dynamic susceptibility collapses on cooling as the sublattice magnetization grows (Fig. 2) due to the combined effect of the proximity to P_x and pressure inhomogeneity.

By comparison to previous data,^{4,18} it must be noticed than in Ref. 4, the temperature variation of the elastic magnetic signal I_M is slow just above P_x , rather steep near 0.8

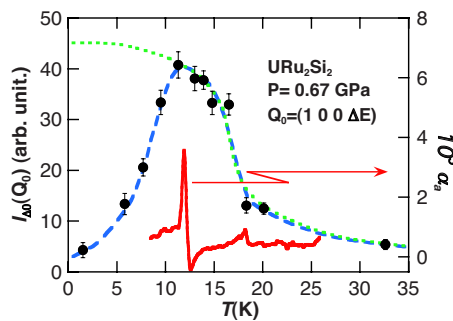


FIG. 5. (Color online) Integration of the dynamic susceptibility $I_{\Delta_0}(\mathbf{Q}_0)$ from $E=0.6$ meV \rightarrow $E=2.5$ meV (black circles). The dashed blue curve is a guide for the eyes. Thermal expansion in red (solid line). If the HO persists down to 0 K, its contribution, measured at $P=0$ in Ref. 25, is the extrapolated green dotted line.

GPa and again slow at 1 GPa. In Ref. 18, for the same pressure of 1 GPa, I_M has a steeper T dependence than in Ref. 4. All these data indicate a high sensitivity to the pressure inhomogeneity. Assuming that I_M and $I_{\Delta_0}(\mathbf{Q}_0)$ reflect, respectively, the AF fraction and the HO fraction, we can assert that at least 95% of the antiferromagnetic phase is achieved at 1.5 K. This evaluation confirms the conclusion of a recent report.³⁶

Our result at $P=0.67$ GPa is that the main feature of URu_2Si_2 occurs for both hidden order and antiferromagnetic phases at the wave vector \mathbf{Q}_0 with sharp excitations in the hidden order phase and a large elastic magnetic signal in the antiferromagnetic state; the excitation collapses at low temperature in the antiferromagnetic state. It is worthwhile to notice that this wipe out at P_x coincides with the disappearance of bulk superconductivity.¹⁹ It was proposed in the framework where the hidden order is quadrupolar⁹ that the strong excitations describe the longitudinal fluctuations of a magnetic dipole in the hidden order phase, whereas inside the antiferromagnetic phase, the inelastic neutron scattering signal coming from quadrupolar fluctuations is not measurable by neutron scattering.

The observation of the excitation Δ_1 at \mathbf{Q}_1 even in the antiferromagnetic phase appears correlated with the persistence of nesting through P_x derived from transport measurements. Without nesting, the system will end up in the paramagnetic ground state. The loss of electronic carriers at T_0 or T_N changes the damped response at \mathbf{Q}_0 and \mathbf{Q}_1 in the paramagnetic state to well-defined resonances below the onset of the long-range ordering. \mathbf{Q}_0 seems to be the ordered wave vector for both hidden order and antiferromagnetic phases. In the hypothetical case of a switch from a spin density wave state at \mathbf{Q}_1 to an antiferromagnetic state at \mathbf{Q}_0 above P_x , it is expected to be accompanied by a drastic change of the excitations at \mathbf{Q}_1 and for transport measurements; this is not observed.

It is worthwhile to compare URu_2Si_2 , where the exotic properties originate from the $5f^2$ configuration of the U atoms, with new Pr skutterudite systems, where the key electrons belong to the $4f^2$ configuration. The situation of URu_2Si_2 at T_0 seems to be similar to that reported for $\text{PrFe}_4\text{P}_{12}$ (Refs. 23, 37, and 38) with regard to the concomitant effect of nesting and HO parameter at the ordering temperature T_A . Furthermore, it is interesting to mention that in $\text{PrFe}_4\text{P}_{12}$, it has been established that a switch from HO to AF state occurs at $P_x \sim 2$ GPa, the key wave vector being $\mathbf{Q}=(1,0,0)$ for both HO and AF phases.³⁹ The cubic symmetry is not preserved in the AF phase due to the induced anisotropic magnetization. In URu_2Si_2 , AF order leads to a doubling of the unit cell, which can induce a reduction of the charge carrier number at the Fermi level. As de Haas-van Alphen measurements show that the Fermi surface does not change significantly up to 1.7 GPa at low temperature, we conclude that the HO phase also has a unit cell twice as large.

To conclude, our experiments point out the drastic change in the response of the inelastic neutron scattering at \mathbf{Q}_0 precisely at the transition from hidden order to antiferromagnetism. The low-energy resonance at \mathbf{Q}_0 is a signature of the hidden order phase. The invariance of \mathbf{Q}_0 in HO and AF

phases is strongly supported by the invariance of quantum oscillations through P_x and P^* .⁴⁰ Another issue will be to precise the band structure in the different phases depending of the hypothesis on the localization of the $5f$ electrons in order to clarify the Fermi surface nesting. Finally, our observation of a specific resonance associated with an ordering

may enter in the same class of phenomena than the resonance observed in unconventional superconductors (see recently Ref. 41).

This work is supported by the Agence Nationale de la Recherche through Contract No. ANR-06-BLAN-0220.

*frederic.bourdarot@cea.fr

- ¹P. Chandra, P. Coleman, J. A. Mydosh, and V. Tripathi, *Nature (London)* **417**, 831 (2002).
- ²Y. Kuramoto and K. Miyake, *Prog. Theor. Phys.* **1**, 60 (2005).
- ³V. Aji and C. M. Varma, *Phys. Rev. B* **75**, 224511 (2007).
- ⁴H. Amitsuka, K. Matsuda, I. Kawasaki, K. Tenya, and M. Yokoyama, *J. Magn. Magn. Mater.* **310**, 214 (2007).
- ⁵M. B. Maple, J. W. Chen, Y. Dalichaouch, T. Kohara, C. Rossel, M. S. Torikachvili, M. W. McElfresh, and J. D. Thompson, *Phys. Rev. Lett.* **56**, 185 (1986).
- ⁶H. Ikeda and Y. Ohashi, *Phys. Rev. Lett.* **81**, 3723 (1998).
- ⁷V. P. Mineev and M. E. Zhitomirsky, *Phys. Rev. B* **72**, 014432 (2005).
- ⁸P. Santini and G. Amoretti, *Phys. Rev. Lett.* **73**, 1027 (1994).
- ⁹F. J. Ohkawa and H. Shimizu, *J. Phys.: Condens. Matter* **11**, L519 (1999).
- ¹⁰K. Hanzawa, *J. Phys.: Condens. Matter* **19**, 072202 (2007).
- ¹¹A. Kiss and P. Fazekas, *Phys. Rev. B* **71**, 054415 (2005).
- ¹²L. P. Gor'kov and A. Sokol, *Phys. Rev. Lett.* **69**, 2586 (1992).
- ¹³C. M. Varma and L. Zhu, *Phys. Rev. Lett.* **96**, 036405 (2006).
- ¹⁴K. Matsuda, Y. Kohori, T. Kohara, K. Kuwahara, and H. Amitsuka, *Phys. Rev. Lett.* **87**, 087203 (2001).
- ¹⁵S. Takagi, S. Ishihara, S. Saitoh, H. I. Sasaki, H. Tanida, M. Yokoyama, and H. Amitsuka, *J. Phys. Soc. Jpn.* **76**, 033708 (2007).
- ¹⁶A. Amato, M. J. Graf, A. de Visser, H. Amitsuka, D. Andreica, and A. Schenck, *J. Phys.: Condens. Matter* **16**, S4403 (2004).
- ¹⁷G. Motoyama, T. Nishioka, and N. K. Sato, *Phys. Rev. Lett.* **90**, 166402 (2003).
- ¹⁸F. Bourdarot, A. Bombardi, P. Burllet, M. Enderle, J. Flouquet, P. Lejay, N. Kernavanois, V. P. Mineev, L. Paolasini, M. E. Zhitomirsky, and B. Fak, *Physica B* **359-361**, 986 (2005).
- ¹⁹E. Hassinger, G. Knebel, K. Izawa, P. Lejay, B. Salce, and J. Flouquet, *Phys. Rev. B* **77**, 115117 (2008).
- ²⁰T. Kohara, Y. Kohori, K. Asayama, Y. Kitaoka, M. B. Maple, and M. S. Torikachvili, *Solid State Commun.* **59**, 603 (1986).
- ²¹W. Schlabitz, J. Baumann, B. Pollit, U. Rauchschwalbe, H. M. Mayer, U. Ahlheim, and C. D. Bredl, *Z. Phys. B: Condens. Matter* **62**, 171 (1986).
- ²²O. O. Bernal, C. Rodrigues, A. Martinez, H. G. Lukefahr, D. E. MacLaughlin, A. A. Menovsky, and J. A. Mydosh, *Phys. Rev. Lett.* **87**, 196402 (2001).
- ²³E. Hassinger, J. Derr, J. Levallois, D. Aoki, K. Behnia, F. Bourdarot, G. Knebel, C. Proust, and J. Flouquet, *J. Phys. Soc. Jpn.* **77**, Suppl. A, 172 (2008).
- ²⁴C. R. Wiebe, G. M. Luke, Z. Yamani, A. A. Menovsky, and W. J. L. Buyers, *Phys. Rev. B* **69**, 132418 (2004).
- ²⁵F. Bourdarot, Ph.D. thesis, University Joseph Fourier, 1994.
- ²⁶C. Broholm, J. K. Kjems, W. J. L. Buyers, P. Matthews, T. T. M. Palstra, A. A. Menovsky, and J. A. Mydosh, *Phys. Rev. Lett.* **58**, 1467 (1987).
- ²⁷C. Broholm, H. Lin, P. T. Matthews, T. E. Mason, W. J. L. Buyers, M. F. Collins, A. A. Menovsky, J. A. Mydosh, and J. K. Kjems, *Phys. Rev. B* **43**, 12809 (1991).
- ²⁸F. Bourdarot, B. Fak, K. Habicht, and K. Prokes, *Phys. Rev. Lett.* **90**, 067203 (2003).
- ²⁹C. R. Wiebe, J. A. Janik, G. J. MacDougall, G. M. Luke, J. D. Garrett, H. D. Zhou, Y. J. Jo, L. Balicas, Y. Qiu, J. R. D. Copley, Z. Yamani, and W. J. L. Buyers, *Nat. Phys.* **3**, 96 (2007).
- ³⁰N. H. van Dijk, F. Bourdarot, J. C. P. Klaasse, I. H. Hagemus, E. Bruck, and A. A. Menovsky, *Phys. Rev. B* **56**, 14493 (1997).
- ³¹F. Bourdarot, B. Fak, V. P. Mineev, M. E. Zhitomirsky, N. Kernavanois, S. Raymond, P. Burllet, F. Lapierre, P. Lejay, and J. Flouquet, arXiv:cond-mat/0312206 (unpublished).
- ³²H. Amitsuka, M. Yokoyama, K. Tenya, T. Sakakibara, K. Kuwahara, M. Sato, N. Metoki, T. Honma, Y. Onuki, S. Kawarazaki, Y. Miyako, S. Ramakrishnan, and J. A. Mydosh, *J. Phys. Soc. Jpn.* **69**, Suppl. A, 5 (2000).
- ³³N. Metoki, Y. Koike, Y. Haga, T. Honma, M. Sato, Y. Onuki, N. Kimura, K. Maesawa, H. Amitsuka, M. Yokoyama, K. Kuwahara, and Y. Miyako, *Physica B* **280**, 362 (2000).
- ³⁴A. Villaume, D. Aoki, Y. Haga, G. Knebel, R. Boursier, and J. Flouquet, *J. Phys.: Condens. Matter* **20**, 015203 (2008).
- ³⁵F. Bourdarot, B. Fak, V. P. Mineev, M. E. Zhitomirsky, N. Kernavanois, S. Raymond, F. Lapierre, P. Lejay, and J. Flouquet, *Physica B* **350**, e179 (2004).
- ³⁶H. Amitsuka, K. Matsuda, M. Yokoyama, I. Kawasaki, S. Takayama, Y. Ishihara, K. Tenya, N. Tatelwa, T. C. Kobayashi, and H. Yoshizawa, *Physica B* **403**, 925 (2008).
- ³⁷J. G. Park, D. T. Adroja, K. A. McEwen, M. Kohgi, K. Iwasa, and Y. S. Kwon, *Physica B* **359-361**, 868 (2005).
- ³⁸M. Kohgi, K. Iwasa, and K. Kuwahara, *Physica B* **385-386**, 23 (2006).
- ³⁹H. Hidaka, I. Ando, H. Kotegawa, T. C. Kobayashi, H. Harima, M. Kobayashi, H. Sugawara, and H. Sato, *Phys. Rev. B* **71**, 073102 (2005).
- ⁴⁰H. Harima (private communication).
- ⁴¹C. Stock, C. Broholm, J. Hudis, H. J. Kang, and C. Petrovic, *Phys. Rev. Lett.* **100**, 087001 (2008).